AIMS Energy, 13(2): 428–448.
DOI: 10.3934/energy.2025016
Received: 10 November 2024
Revised: 16 March 2025
Accepted: 25 March 2025
Published: 14 April 2025

https://www.aimspress.com/journal/energy

Research article

Experimental investigation of the effect of TDS on the thermal performance of the different types of solar stills

Hind I. El-Refaey[1,*], Saleh. M. Shalaby[2], Swellam W. Sharshir[3], Hewida Omara[1] and Tamer A. Gado[1]

[1] Irrigation and Hydraulics Engineering Department, Faculty of Engineering, Tanta University, Tanta 31511, Egypt
[2] Engineering Physics and Mathematics Department, Faculty of Engineering, Tanta University, Tanta, 31511, Egypt
[3] Mechanical Engineering Department, Faculty of Engineering, Kafrelsheikh University, Kafrelsheikh 33516, Egypt

* **Correspondence:** Email: helrefaey369@gmail.com, Hind152602@f-eng.tanta.edu.eg; Tel: +201557207300.

Abstract: In regions with a restricted availability of drinkable water, solar stills offer a solution for a passive solar desalination method. In this study, three designs for solar stills are examined: the conventional solar still (CSS), the hemispheric solar still (HSS), and the pyramidal solar still (PSS). The experimental investigations were conducted over three consecutive days, thereby varying the total dissolved solids (TDS) concentrations in the basin water at 1000, 2000, and 3000 ppm. A comparative analysis focused on the performance of the various solar stills and the impact of TDS variation. The results revealed that the PSS consistently outperformed the CSS and HSS across all TDS levels. Notably, the PSS exhibited superior daily energy and exergy efficiencies. Furthermore, the daily productivity and energy efficiencies displayed an inverse relationship with the TDS concentration. A cost analysis indicated that the PSS achieved the lowest distilled water price, reaching a value of 0.0151 $/L. Specifically, the PSS exhibited a 17.3% and 3.5% higher accumulated daily productivity compared to CSS and HSS, respectively, at TDS = 1000. However, at TDS = 3000, the daily productivity of the PSS decreased by 3.5% and 7.5% compared to TDS = 2000 and 1000, respectively. Similarly, the energy efficiency of the PSS decreased by 5.27% and 8.67% as the TDS increased from 1000 to 3000. Notably, across all solar still types, the lowest cost values were consistently associated with the lowest TDS concentrations, with the PSS yielding the lowest cost overall.

Keywords: solar desalination; pyramid solar still; hemispheric solar still; cost analysis; TDS

1. Introduction

Freshwater is vital for the continuation of life on Earth, whether for human, plant, or animal environments. Humans can survive for several weeks without food, but only a few days without water. The world is facing a water crisis, as just 3% of the Earth water is potable, two-thirds of which is stored in rivers or glacial mountains, and what remains is small and insufficient [1]. Accordingly, governments worldwide are concerned about a number of issues, including the scarcity of drinkable water. The possible reasons for the shortage of freshwater resources are industrialization and the rapid population expansion in the world; thereby, it has led scientists to look for a different approach to satisfy this need [2].

The US Geological Survey classifies salt water into three categories according to its concentration. The first type is the brackish type, where the salt concentration ranges from 1,000–3,000 ppm. The second is the medium-salinity class, where the salt concentration ranges from 3,000–10,000 ppm. The third is the highly salty type, where the salt concentration ranges from 10,000–35,000 ppm [3]. The process of turning this saline water into drinkable water is called desalination. However, this process is known for its high energy consumption. On the other hand, solar energy is a clean energy source that has the potential to grow into a reliable energy source without the need for highly specialized and sophisticated equipment for its widespread use. Furthermore, its use doesn't seem to have any noticeable contaminating impacts. When Austrian Guntur created a solar furnace using mirrors in 1885, a scientific study into the use of sun energy began [4]. Accordingly, solar stills (SSs) have been introduced in order to offer a solution for a passive solar desalination process.

Over the past few years, many modifications have been made to SSs designs. It includes the single slope SS [5], double-slope SS [6], single and double effect SS [7], inclined SS [8], vertical SS [9], triangular SS [10], stepped SS [11], stepped with vertical wick SS [12], corrugated absorber SS [13], tubular SS [14], conical SS [15], spherical SS [16], rotating wick SS [17], corrugated wick SS [18], trapezoidal SS [19], and prism-shaped SS [20]. Other modifications have been conducted to the internal constituents' parts of the SS and some additives. It includes using a sliced absorber plate with a new design of glass cover [21], using an external condenser [22], using the glass cover cooling technique [23], using a thermoelectric cooling system [24], using a PCM (Phase Change Material) [25,26] and a nano-based PCM [22], using sensible heat storage (SHS) materials [5], using an energy storage biomaterial [27], using boulders and fines in biodegradable organic materials [28], using different basin materials [29], using an evacuated flat-plate collector [30], using reflectors [26], using parabolic concentrators [31], using a nano-coated absorber [32], using fins [8] and wick finned absorber [33], using floating porous absorber with different shapes [34], using different materials of the transparent covers [24], using different materials of the absorber plate [35], using industrial wastewater as a basin feed water [36], using geothermal energy [37], and using Fe_3O_4, graphene oxide, and paraffin as nanofluids [38]. Mandev et al. [39] investigated the effect of using a Peltier cooling unit as well as using cellulose papers in the form of hemp and high absorber papers with dark colors on the productivity of the solar still. It was shown that using high-absorbent papers in upright columns patterns improved the daily productivity and the thermal efficiency of the solar still by 60% and 45%, respectively, which were more than that obtained from the conventional solar still. Köse et al. [40]

investigated a horizontal solar still with a plastic transparent cover using a corrugated absorber plate (basin liner), hemp rope, and a cooling-plastic cover mechanism by a water spraying technique. It was outlined that the modified solar still obtained a maximum thermal efficiency of about 4.9% and a maximum instantaneous efficiency of about 10.6%.

A hemispheric solar still (HSS) is a type of SS that is characterized by an almost high efficiency as a result of the hemispherical shape giving a larger condensing area; at the same time, it only occupies a small volume in the experimental field. Elsawy et al. [41] investigated the effect of adding charcoal (CHL) produced from carbonized corncobs and the wood of the guava tree (CCC), and both were treated with activators of HCl and NaOH to the basin water of the HSS. The HSS that used CCC treated with HCl floated in the basin water (lake water) gave the best performance and provided a daily productivity of about 41% more than the conventional CSS. Dahab et al. [42] examined an evacuated tube solar collector integrated to an HSS and tested the impact of the basin water depth, the number of evacuated tubes, and its distribution. It was revealed that the daily productivity of the HSS with 16-evacuated tubes (distributed in all direction of the basin perimeter) and a water thickness of 10 mm gave the highest improvement of 551% over the conventional HSS. Attia et al. [43] investigated an HSS with different cases: with Al foil and P granules, with a Zn sheet and P granules, and with a Cu sheet and P granules. It was concluded that the Cu sheet and P granules showed the best performance, where it gave the better daily productivity improvement of about 62% compared to the conventional HSS. Aluminum waste can be used inside the basin water of an HSS to boost the absorption rate of solar energy and then increase the heat gained by the basin water due to the high conductivity of aluminum [44]. Additionally, aluminum waste is a sensible thermal storage medium to recover heat during the low intensity of solar insolation. Beggas et al. [44] outlined that using aluminum waste within the basin water of the HSS improved the daily yield by about 48.2% over the conventional HSS. Sharshir et al. [45] investigated the V-corrugated-wick basin HSS using two different phase change materials (PCMs): paraffin wax and sheep fat. They proved that using sheep fat as a PCM beneath the corrugated basin covered with a cotton wick elevated the daily yield of the modified HSS by about 40% more than the conventional HSS with a flat absorber.

The use of a corrugated absorber integrated to the pyramidal solar still (PSS) was investigated, and the results showed that the daily yield increased by about 52.5% in contrast to the conventional solar still (CSS) [46]. A CFD (Computational Fluid Dynamics) model was used to analyze the thermal metrics of the PSS [47]. The outcomes showed that the experimental and CFD modeling results agreed rather well. It can be concluded that the CFD model can be employed to forecast the thermal performance of the PSS with a good accuracy. Different types of wick materials (silk, plush, cotton, and jute) have been used within the basin water of the PSS by Abdullah et al. [48]. In addition to the sun, three electric heaters using solar panels were also used to raise the PSS basin water's temperature even further. It was indicated that using jute was the best choice of wick materials with an improvement of 125%, followed by cotton with an improvement of 115%, followed by plush with an improvement of 88%, and finally followed by silk with an improvement of 60% over the PSS without using wick materials. A new design of trapezoidal PSS with a trapezoidal pyramidal wick was explored by Sharshir et al. [49]. It was concluded that the daily output of the trapezoidal PSS using a trapezoidal wick, cover cooling, reflectors, and copper-oxide based nanofluid was improved by 147.3%. Omara et al. [50] announced that the average daily productivity of the convex dish-shape absorber PSS using jute clothes and Ag-based nano-coating to the absorber was improved by 78% more than that of the PSS without any enhancers.

Sharshir et al. [51] investigated the PSS with 5 cases of operation and compared it with the CSS. The effect of using a wick, reflector, cover cooling, and nanofluid with TiO_2 additives on the thermal performance of the pyramidal SS (case 5) was investigated. It was reported that the daily productivity of the PSS with a wick, reflector, cover cooling, and nanoparticle fluid was higher than the daily output of the CSS by 127.3%. Besides, the energy efficiency of the PSS (case 5) was developed by about 121.3% over the CSS. Modi and Gamit [52] investigated the square PSS utilizing energy storage materials (aluminum oxide Al_2O_3 and sodium nitrate $NaNO_3$) as nanoparticles added to the basin water. They proved that using $NaNO_3$ improved the daily yield of the square PSS 5.5% better than using Al_2O_3. Additionally, aluminum oxide Al_2O_3, magnesium oxide AgO, and graphene oxide GO have been used as nanoparticles within the basin water of the PSS [53]. It was shown that using MgO-based nanofluid in the PSS is better than using Al_2O_3-based nanofluid by about 10.4% according to the daily productivity as compared to the conventional PSS. An attempt to enhance the daily yield of the PSS has been conducted using different types of sensible heat storage materials such as quartz rock (0.25-inch and 0.75-inch), mild steel pieces, and sieved red bricks (1-0.25 inch) [54]. In order to improve the thermal performance of the PSS, solid clay pots were utilized as a sensible storage medium [55]. The daily productivity of the PSS using 36 clay pots was improved by 72.44% over the PSS that didn't use clay pots. Analyzing the distillate water quality obtained a total dissolved solids (TDS) of 28 mg/l and a pH of 7.02. These results proved that the distillate water was suitable for human consumption because it met the World Health Organization (WHO) criteria. It was discovered that the PSS's daily yield using 1-0.25 inch red bricks as a sensible storage medium was enhanced by 30% compared to the CSS. Asadabadi and Sheikholeslami [56] investigated the effect of using copper fins integrated to the basin of the PSS as a modified PSS in an attempt to boost the heat transfer rates. The improved PSS's thermal performance was contrasted with the traditional PSS's. It was found that the use of hollow circular copper fins improved the daily productivity by 62.5%. In an attempt to enhance the evaporation rate, Alshqirate et al. [57] inserted palmately leaf as a natural fiber and as a sensible storage medium within the basin water of the PSS. It was outlined that using palmately leaf as a natural fiber increased the daily output of the PSS by 44.5% over the conventional PSS.

Ahmed et al. [58] declared that using cylindrical encapsulated PCM (paraffin wax) fins (4 cm height) integrated to the PSS improved the daily productivity by 44.4% over the CSS. Sudhakar et al. [59] used a paraffin wax as a PCM below the basin of the triangular PSS and double-slope SS. It was found that the daily outputs of the triangular PSS and of the double slope SS were increased by 15.9% and 8.1%, respectively, in contrast to the conventional double slope SS. A comparison between pentagonal PSS and tubular SS with and without crude wax as a PCM has been performed by Bhoopathi et al. [60]. It was confirmed that, without PCM, the tubular SS had a daily yield that was approximately 13.5% higher than the pentagonal PSS's. Furthermore, the daily distillate output of the PCM-modified tubular SS was enhanced by about 7.1% in contrast to the standalone tubular SS without PCM. Using pistachio shell powder (bio-waste) as a sensible storage medium to augment the performance of the tubular SS was covered by Noman and Manokar [61]. It was found that the tubular SS with pistachio shell powder has a daily productivity higher than the conventional tubular SS by about 46.3%. Prasad et al. [62] investigated the square PSS with paraffin as a PCM, and an improvement of about 21.11% was achieved compared to the square PSS without the PCM.

In this work, three different configurations of SSs are created, manufactured, and tested in accordance with Kafrelsheikh City weather conditions. As far as the authors of this work know, there are very few papers that investigated the influence of the TDS within the basin water on the thermal

performance of the solar-driven desalination systems under consideration. Hence, the experimental investigations are conducted over three several days, thereby varying the TDS concentrations in the basin water as 1000, 2000, and 3000 ppm. Furthermore, a comparative analysis is conducted that focuses on the various SSs performance and the impact of TDS variation based on the daily output, cost, energy, and energetic efficiency.

2. Test-rig description and experimental investigation

The three considered SSs (CSS, HSS and PSS) are provided with saline water at the same TDS for each experiment, as seen in Figure 1. The water is fed via a supplying tank insulated with 5 cm thick fiberglass. The experiments were performed within Kafrelsheikh City (30.57 °E, 31.07 °N). The work investigates the effect of various values of TDS of the supplying water on the thermal performance of the considered SSs.

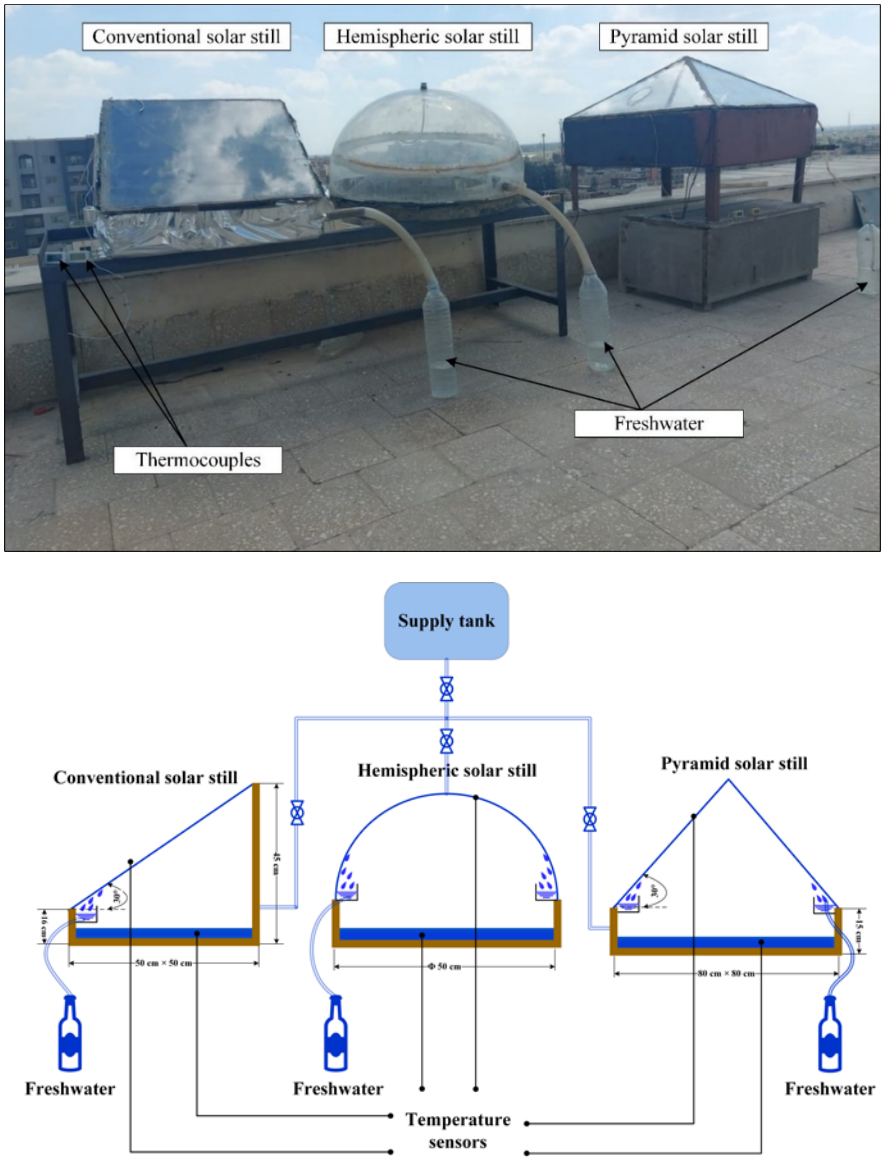

Figure 1. Test-rig representation.

2.1. Conventional solar still (CSS)

The CSS consists of a black painted metallic basin of square area (50 cm × 50 cm) made of a 0.15 cm GI (Galvanized Iron) sheet. The long side is 0.45 m tall and the short side is 0.16 m; thus, the tilt angle of the glass cover (3.5 mm thickness ordinary glass) is approximately 30^o with respect to the horizontal. The system is insulated from the back and sides with 0.05 m thickness of glass wool. At the front end of the cover, there is a collecting channel to gather the distillate and then flow it out to a bottle through a hose.

2.2. Hemispheric solar still (HSS)

The HSS consists of 0.15 cm thick steel basin with a circular-shaped base of diameter of 0.5 m (0.20 m^2 area). The inner surface of the metallic basin is painted with ordinary black matt to maximize the absorbed solar radiation. The basin is totally insulated with a good insulator rubber of 1.2 mm thick to minimize the heat loss to the surroundings. The transparent cover as a condenser is a hemispherical dome fabricated from acrylic with a circular-shaped base of diameter 0.5 m. The distilled water is collected via a channel built in the acrylic cover. A port of diameter 1 cm is drilled in the transparent cover to feed the basin with saline water.

2.3. Pyramidal solar still (PSS)

The pyramidal solar still (PSS) consists of a black-coated basin of a square-shaped base-area of 80 cm × 80 cm made of 0.15 cm thick steel. The basin has an equal height of all sides of 0.15 m and the exterior is insulated with 0.05 m of glass wool. The condensing glass cover is composed of four glass plates of a triangle shape to form a pyramidal shape. The three SSs—CSS, PSS, and HSS—underwent a 24-hour leakage test to ensure zero water or vapor leakage.

2.4. Experimental procedures and uncertainty

The experiments took place on three closed days during the summer of 2023. On the first day, the three SSs (CSS, HSS and PSS) were tested, where the three SSs contained the same mass of basin water as TDS = 1000. On the second day, TDS = 2000, while on the third day, TDS = 3000. During the experiments, a group of variables were measured, and readings were captured hourly from 9 am to 6 pm. The cover's temperature, basin water temperature, sun radiation, ambient temperature, and absorb plate temperature were all recorded. Every hour, the volume of distilled water was measured using the calibrated flask. The characteristics of the measurement tools are presented in Table 1, where the uncertainty (u) is measured according to the following formula [63]:

$$u = \frac{a}{\sqrt{3}} \tag{1}$$

Table 1. Measurement tools and its properties.

Instrument	Property	Unit	Model	Range (R)	Accuracy (a)	Uncertainty (u)
Calibrated flask	Water volume	ml	--	0–2000	± 2	1.155
Thermocouple	Temperature	℃	Type-K	–20–120	± 0.1	0.06
Solar Radiation Meter	Solar radiation	W/m^2	TES-1333R	0–5000	± 10	5.77
Anemometer	Wind speed	m/s	GM816	0.4–30	± 0.1	0.06
Measuring tape	Dimensions	m	--	0–5	± 0.1	0.06

3. Thermal analysis

The thermal analysis was performed to the SSs using the collected measured data for each solar still during the experimental period. The concept "thermal performance" represents the thermal behavior of the solar still, whether in positive or negative manner, and it is expressed in terms of energy (thermal) and exergetic efficiency.

3.1. Energy efficiency

The energy efficiency of SS is the quantity of water produced per unit area for a certain value of solar insolation. Since the amount of distilled water and solar insolation change hourly throughout the day, the hourly energy efficiency (η_{h-en}) must be calculated; then, the value is collected to become the daily energy efficiency (η_{d-en}). The hourly energy efficiency can be calculated as follows [51,64]:

$$\eta_{h-en} = \frac{P_h \times L_{ev}}{[I_h \times A] \times 3600} \tag{2}$$

$$L_{ev} = (2501900) - (2407.06 \times T_w) + (1.192217 \times T_w^2) - (0.015863 \times T_w^3) \tag{3}$$

where T_W denotes the water temperature

The hourly productivity (P_h), measured in kg/hr, represents the hourly productivity. The latent heat of vaporization (L_{ev}) is typically measured in J/kg. The hourly value of solar insolation (I_h) quantifies the amount of energy received per unit area within an hour and is commonly expressed in W/m^2. The area (A) denotes the total area covered by water in a basin and is typically measured in m^2.

The daily productivity (P_d) of a solar still is calculated as follows:

$$P_d = \sum P_h \tag{4}$$

Then, the daily energy efficiency (η_{d-en}) is as follows [65,66]:

$$\eta_{d-en} = \frac{\sum (P_h \times L_{ev})}{\sum ([I_h \times A] \times 3600)} \tag{5}$$

3.2. Exergy efficiency

Exergetic efficiency determines how effectively a system utilizes its available energy to perform useful work; in other words, is defines the system closeness to the ideality. The hourly exergy

efficiency (η_{h-ex}) and daily exergy efficiency (η_{d-ex}), based on the entire day's working hours, are determined as follow [65–67]:

$$Ex_i = [I_h \times A] \times \left[1 - \frac{4}{3} \times \left(\frac{T_a}{T_s}\right) + \frac{1}{3} \times \left(\frac{T_a}{T_s}\right)^4\right] \quad (6)$$

$$Ex_o = \frac{P_h \times L_{ev}}{3600} \times \left(1 - \frac{T_a}{T_w}\right) \quad (7)$$

$$\eta_{h-ex} = \frac{Ex_o}{Ex_i} \quad (8)$$

$$\eta_{d-ex} = \frac{\sum Ex_o}{\sum Ex_i} \quad (9)$$

The hourly exergy input (E_{xi}) and output (E_{xo}) represent the energy supplied to and produced by a system within an hour, respectively, and are measured in joules. The ambient air temperature (T_a) is measured in kelvin and indicates the surrounding temperature, while the sun-surface temperature (T_s), which is often assumed to be 6000 kelvins, serves as a source temperature for systems exposed to solar radiation.

3.3. Cost estimation

It is important in the SS design to take the lowest cost with the highest efficiency and daily productivity of distilled water into account so that the cost per liter of distilled water is as low as possible. In the following cost analysis model, it was considered that the number of off-days is about 45 days; therefore, the number of annual operating days is about 320 days. The maintenance process includes repainting, checking the insulation and leakage, removing the deposited salt at the basin, cleaning the still from dust, etc.... The scrap value represents the device's worth at the end of its useful life. The subsequent variables that impact the SSs' cost analysis are stated as follows [68,69]:

$$SFF = i/[(1+i)^n - 1] \quad (10)$$

$$CRF = (SFF) \times (1+i)^n \quad (11)$$

$$FAC = FC \times (CRF) \quad (12)$$

$$SV = 0.2 \times FC \quad (13)$$

$$ASV = (SFF) \times SV \quad (14)$$

$$AMC = 0.15 \times FAC \quad (15)$$

$$AC = FAC + AMC - ASV \quad (16)$$

$$AY = P_d \times N \quad (17)$$

$$CPL = AC/AY \quad (18)$$

where the sinking fund factor (SFF) is a dimensionless parameter used in financial calculations. The yearly interest (i) is taken as 12% per year. The useful life (n) is taken as 10 years. FAC represents the fixed annual cost, while fc denotes the total fixed cost. SV stands for salvage value, and ASV is the

annual worth of the salvage value. AMC refers to the yearly maintenance fee, and AC represents the annual expenses. CPL signifies the water price in ($/L), while AY represents the annual yield in liters. N denotes the annual operating days, which is assumed to be 320 days.

4. Results and discussion

4.1. Analyzing ambient conditions and temperature distribution

Figure 2 represents the surrounding circumstances (temperature and solar radiation) for the experiment days. As the experiment was held on closed days, minor deflections were observed. Reflecting this, the average daily solar radiation varied between 669 and 679 W/m^2, with a standard deviation of 5.63 W/m^2. In the same way, the ambient temperature exhibited a daily average value between 33.1 and 34.3 ℃ at a standard deviation of 0.69 ℃.

Figures 3(a,b), and c display the cover and the water temperature for the CSS, HSS, and PSS. When TDS = 1000 on June 25, 2023, it is found that the various temperature distributions follow the hourly distribution of the incident sun radiation all day long, where the highest value of solar radiation was at 1 pm. Additionally, it was noticed that the average water temperature was 53, 55, and 56 ℃ for the CSS, HSS, and PSS, respectively, whereas the average water temperature was 53.7, 54, and 56 ℃ for the CSS, HSS, and PSS, respectively, when the TDS = 2000 on June 28, 2023. The average basin water temperature was 53, 53, and 56 ℃ for the CSS, HSS, and PSS, respectively, when the TDS = 3000 on July 2, 2023. It can be concluded that the PSS's water temperature was always higher than that of the CSS and HSS in the three cases of TDS, which indicates that the PSS performs better than the CSS and HSS. Furthermore, the glass temperature rapidly declined for the PSS and HSS compared to the CSS due to the larger cover area, which provides a larger heat transfer area.

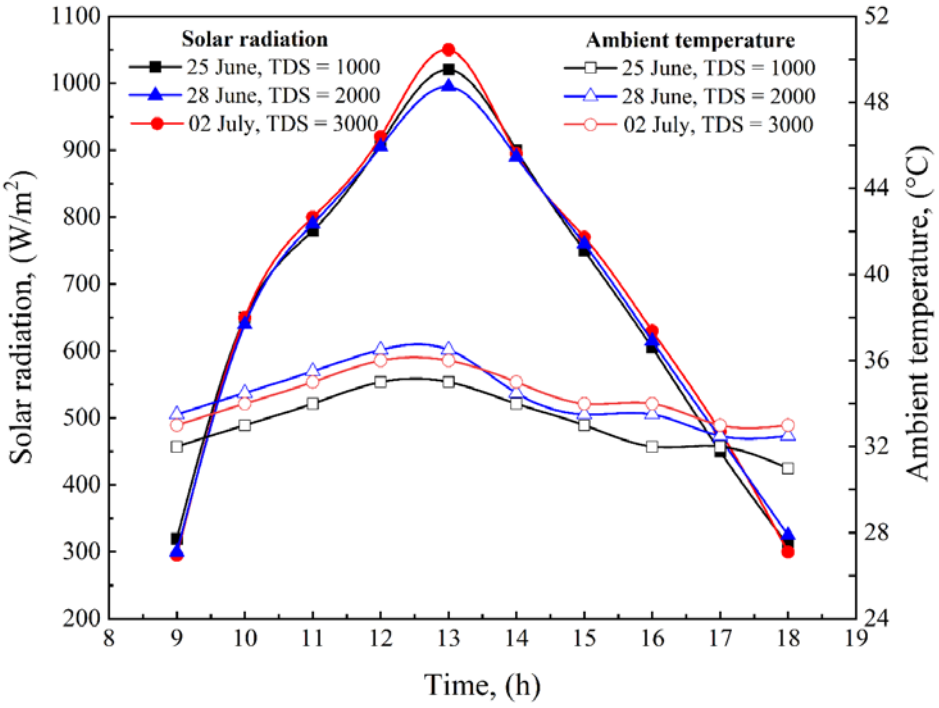

Figure 2. The ambient conditions (temperature and solar insulation) during the experiment days.

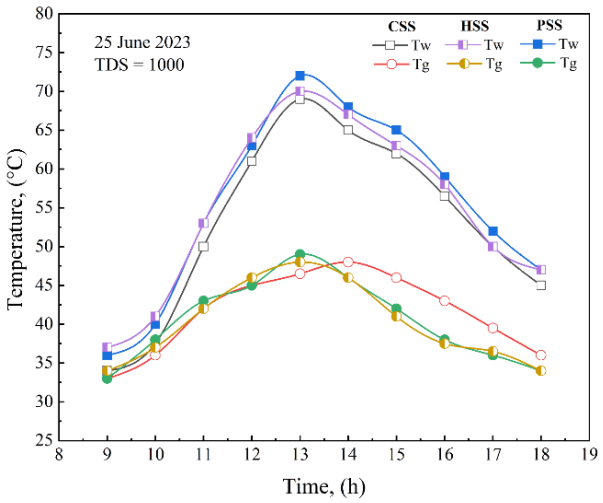

(a)

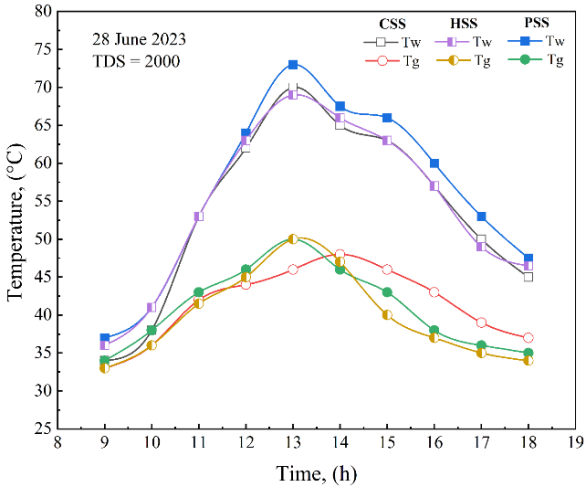

(b)

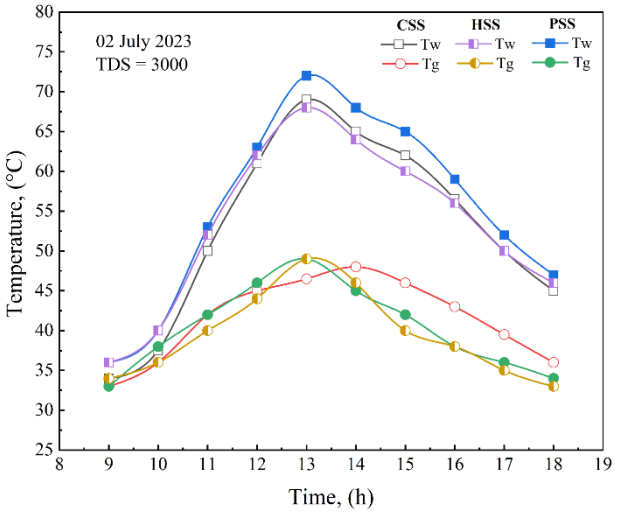

(c)

Figure 3. Temperature of the cover, and water, for the conventional (CSS), hemispheric (HSS), and pyramidal (PSS) SSs during the experiment days.

4.2. Effect of TDS on accumulated daily productivity

In an attempt to ascertain the superiority of the particular type of SSs tested, the hourly propagation of the accumulated daily yield of the three SSs (CSS, HSS and PSS) are plotted when the TDS was 1000, 2000, and 3000, as shown in Figure 4. It can be inferred that the accumulated yield in the case of the PSS was higher than the CSS's and HSS's in all three cases. The accumulated yield of the PSS was higher than the CSS's and HSS's by about 17.3% and 3.5%, respectively, when the TDS is 1000. The increment in the accumulated daily productivity of the PSS was about 16.6% and 3.3% compared to the CSS and the HSS, respectively, when the TDS is 2000. When the TDS is 3000, the accumulated daily productivity of the PSS was found to be higher than the CSS's and HSS's by about 14.9% and 4.7%, respectively. From the analyzed results presented above, it is concluded that the PSS was better than the CSS and HSS in all cases of the investigated TDS.

On the other hand, the accumulated productivity decreases with increasing the TDS values. The daily output linearly decreases when the TDS is raised. The daily productivity of the PSS when the TDS = 3000 decreased by about 3.5% and 7.5% compared to the daily productivity at TDS = 2000 and 1000, respectively. These results are justified by the fact that the more salt or any other solvent added to the water, the higher the boiling point. That is, increasing the dissolved salts in the water delays the evaporation of water depending on the amounts of dissolved salts. Therefore, it can be summarized that the daily productivity is inversely proportional to the TDS, and using lower values of TDS is better to achieve a higher distilled water productivity of a SS. Table 2 presents the hourly and daily productivities of the SSs at the different values of the TDS.

Table 2. Hourly (P_h) and daily (P_d) productivities of the investigated solar stills at different values of TDS.

	TDS = 1000			TDS = 2000			TDS = 3000		
	P_h (kg/m^2)			P_h (kg/m^2)			P_h (kg/m^2)		
Time (h)	CSS	HSS	PSS	CSS	HSS	PSS	CSS	HSS	PSS
9	0.00	0.00	0.00	0.00	0.00	0.00	0.00	0.00	0.00
10	0.14	0.24	0.25	0.16	0.22	0.24	0.15	0.20	0.22
11	0.26	0.33	0.32	0.28	0.30	0.30	0.28	0.28	0.30
12	0.33	0.46	0.48	0.40	0.45	0.46	0.38	0.44	0.44
13	0.41	0.64	0.65	0.56	0.62	0.64	0.53	0.58	0.62
14	0.61	0.57	0.58	0.49	0.56	0.55	0.48	0.56	0.52
15	0.51	0.42	0.45	0.38	0.42	0.42	0.40	0.40	0.42
16	0.4	0.36	0.38	0.32	0.36	0.37	0.30	0.34	0.36
17	0.23	0.26	0.28	0.20	0.22	0.26	0.20	0.20	0.24
18	0.17	0.19	0.20	0.16	0.18	0.20	0.17	0.17	0.20
P_d	3.06	3.47	3.59	2.95	3.33	3.44	2.89	3.17	3.32
Total solar radiation	7365 W/m^2			7359 W/m^2			6790 W/m^2		

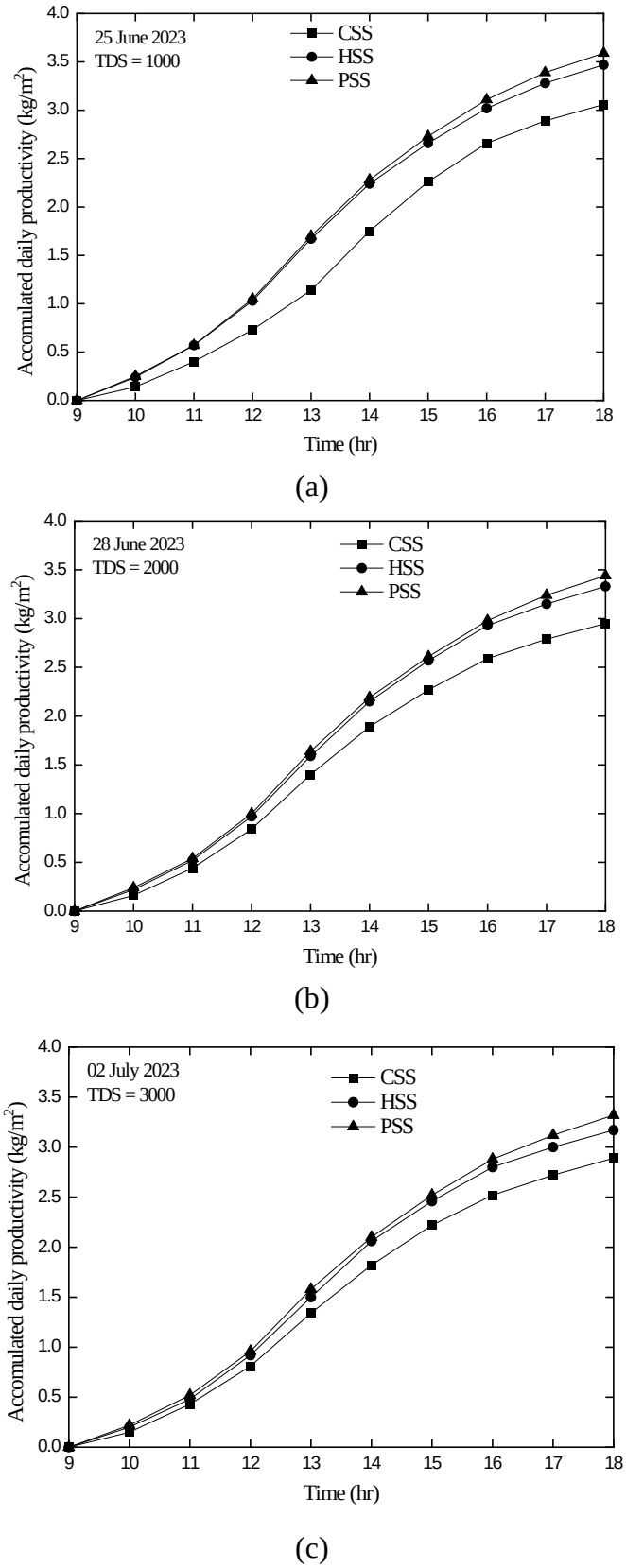

Figure 4. The hourly propagation of the accumulated daily yield of the three SSs (CSS, HSS and PSS) during the experiment days.

4.3. Effect of TDS on energy and exergetic efficiency

The term of energy or exergy efficiencies is an important parameter which shows how far the solar distiller is a good choice. Figure 5a displays the variations of the daily energy efficiency values for the CSS, HSS, and PSS when the TDS values are 1000, 2000, and 3000. Obviously, the daily energy efficiency values increase starting from the CSS, passing through the HSS, and ending with the PSS at the different values of TDS (1000, 2000 and 3000). The PSS has the highest daily energy efficiency value compared to the CSS and HSS with an increment ratio of 16.01% on average compared to the CSS and 3.63% on average compared to the HSS.

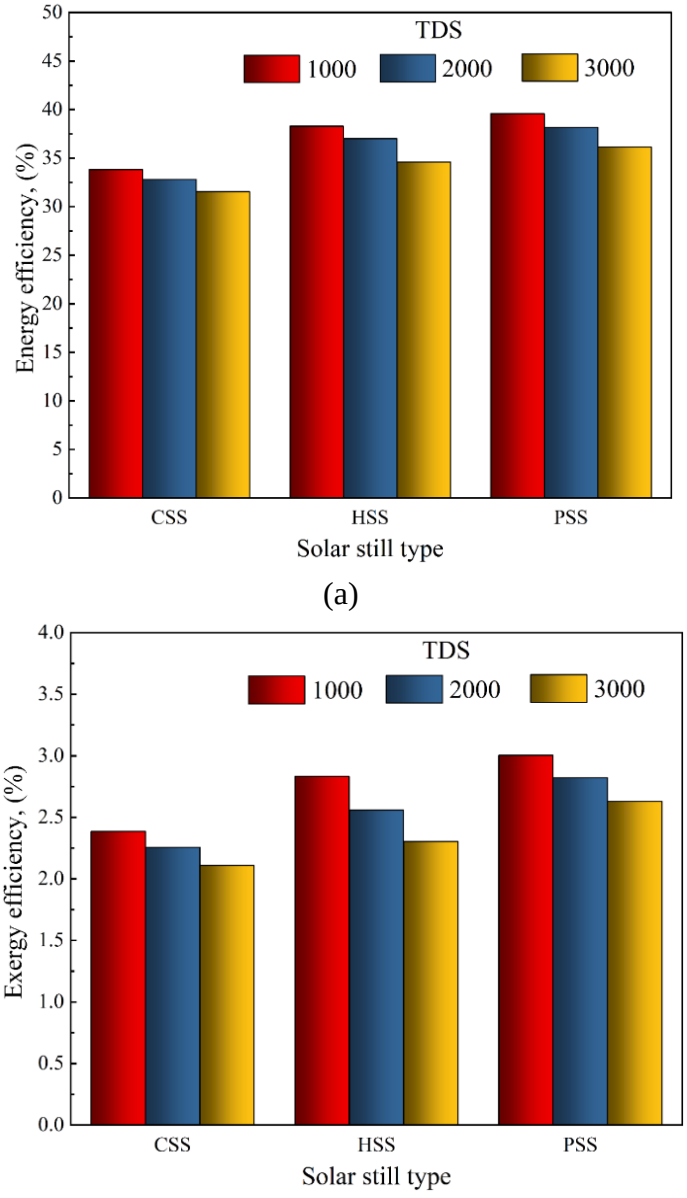

Figure 5. Variations of the (a) daily energy and (b) daily exergetic efficiency of the different solar stills with when TDS = 1000, 2000 and 3000.

Moreover, the variations of the daily exergetic efficiency as a function of the type of SS at different values of TDS are plotted in Figure 5b. The daily exergy efficiency increases in a similar manner, starting with the CSS, passing through the HSS, and ending with the PSS. The highest daily exergy efficiency occurred with the PSS in contrast to the other SSs. The daily exergy efficiency of the PSS is higher by about 25.33% on average than that of the CSS, whereas it exceeds the HSS by about 10.16% on average for all cases of the TDS. It can be concluded that the PSS obtains a better performance in contrast to the performance of the CSS and HSS for all investigated values of the TDS. It is obviously shown that the η_{d-en} and η_{d-ex} linearly decreases with increasing TDS. The η_{d-en} of the PSS when the TDS = 3000 decreases by about 5.27% and 8.67% compared to that when the TDS = 2000 and 1000, respectively. The reduction ratio of η_{d-ex} is 6.74% and 12.33% when the TDS decreases from 3000 to 2000 and 1000, respectively. Thus, it can be said that the η_{d-en} and η_{d-ex} of the PSS are inversely proportional to the TDS.

4.4. Economic analysis

In order to compare the distilled water prices for each of the investigated SSs, the above model (Eqs 10–18) is applied using the Excel program and the obtained results and the annual productivities are given in Table 3. The lowest CPL is obtained at the lowest TDS values for all the three investigated SSs. It should be noted from Table 4 that the lowest value for the CPL yielded from the PSS was about 0.0151 $/L at the TDS = 1000, followed by 0.0156 $/L for the HSS at the TDS = 1000.

Finally, Table 4 offers a comparative analysis of three types of SSs: CSS, HSS, and PSS. Each type was assessed at various TDS levels, thus providing insights into the daily yield, energy efficiency, exergetic efficiency, and CPL. Notably, the PSS emerges as the top performer across all metrics. For instance, at a TDS level of 1000, the PSS achieves an impressive daily output of 3.59 L/m², accompanied by energy and exergetic efficiency of 39.58% and 3.00%, respectively. Remarkably, despite its superior performance, the PSS also exhibits the lowest CPL, priced at 0.0151 $/L. In contrast, the HSS yields 3.47 L/m² with a thermal efficiency of 38.29% and an exergetic efficiency of 2.83%, albeit at a slightly higher cost of 0.0156 $/L. Meanwhile, the CSS lags behind both the PSS and HSS in the performance metrics, resulting in the highest cost per liter at 0.0177 $/L due to its lower daily output of 3.06 L/m² and thermal efficiency of 33.82%.

Table 3. Comparison of cost analysis for the various the various investigated solar stills.

Parameter	TDS	CSS	HSS	PSS
FC ($)		90	90	90
FAC ($)		15.93	15.93	15.93
AMC ($)		2.389	2.389	2.389
ASV ($)		1.03	1.03	1.03
AC ($)		17.29	17.29	17.29
AY (L)	1000	979.2	1110.4	1148.8
	2000	944.0	1065.6	1100.8
	3000	924.8	1014.4	1062.4
CPL ($/L)	1000	0.0177	0.0156	0.0151
	2000	0.0183	0.0162	0.0157
	3000	0.0187	0.0170	0.0163

Table 4. Comparative analysis of CSS, HSS, and PSS solar stills at different TDS levels.

Type	TDS	Daily output, (L/m^2)	Energy efficiency, (%)	Exergy efficiency, (%)	Cost, ($/L)
CSS	1000	3.06	33.82	2.38	0.0177
	2000	2.95	32.79	2.26	0.0183
	3000	2.89	31.54	2.11	0.0187
HSS	1000	3.47	38.29	2.83	0.0156
	2000	3.33	37.01	2.56	0.0162
	3000	3.17	34.60	2.30	0.017
PSS	1000	3.59	39.58	3.00	0.0151
	2000	3.44	38.16	2.82	0.0157
	3000	3.32	36.15	2.63	0.0163

5. Conclusions and future work

In this paper, three types of SSs were tested: the CSS, HSS, and PSS. The three systems were tested by conducting experiments over three closed days in the summer, where the TDS values were 1000, 2000, and 3000. The systems were assessed based on the daily output, cost, energy, and exergetic efficiency. From analyzing the results, a set of important conclusions were obtained as follows.

- The best value of the accumulated daily productivity was obtained for the PSS, and it was higher than the CSS's and the HSS's by about 17.3% and 3.5%, respectively, at the TDS = 1000.
- The daily productivity of the PSS when the TDS = 3000 decreased by about 3.5% and 7.5% compared to the daily productivity at the TDS = 2000 and 1000, respectively.
- The energy efficiency of the PSS when the TDS = 3000 decreased by about 5.27% and 8.67% compared to that at the TDS = 2000 and 1000, respectively.
- The reduction ratio of exergy efficiency was 6.74% and 12.33% when the TDS decreased from 3000 to 2000 and 1000, respectively.
- The lowest value of the *CPL* of distilled water was obtained at the lowest values of the TDS for all CSS, HSS, and PSS. The lowest value ever for the *CPL* was yielded from the PSS and was about 0.0151 $/L.

Through the results obtained in this work, it can be confirmed that these results are correct and achieved within the limitations of climatic conditions of Kafr El-Sheikh city in Egypt, and it is possible to obtain better results in other places in the world under other different climatic conditions. For the future, it is recommended to use the PSS because of its higher thermal performance compared to the HSS and CSS studied in this work. Moreover, the present study could be completed in the future but over a larger range of TDS values to demonstrate and draw more comprehensive conclusions. Additionally, one should study the system's performance throughout the year to determine the impact of different weather factors on the proposed system.

Use of AI tools declaration

The authors declare that they have not used Artificial Intelligence (AI) tools in the creation of this article.

Conflict of interest

The authors declare that they have no known competing financial interests or personal relationships that could have appeared to influence the work reported in this paper.

Author contributions

The authors confirm contribution to the paper as follow: Hind I. El-Refaey (Corresponding author): Formal analysis, Investigation, Methodology, Writing—original draft, Visualization, Software, Resources; Saleh M. Shalaby: Methodology, Investigation, Visualization, Writing—review & editing, Resources, Supervision; Swellam W. Sharshir: Conceptualization, Methodology, Writing—review & editing, Resources; Hewida Omara: Writing—review & editing, Investigation, Data curation, Supervision; and Tamer A. Gado: Methodology, Writing—review & editing, Resources, Supervision.

References

1. Duffie JA, Beckman WA (2013) *Solar Engineering of Thermal Processes*. *John Wiley & Sons*. https://doi.org/10.1002/9781118671603
2. Kandeal AW, Joseph A, Elsharkawy M, et al. (2022) Research progress on recent technologies of water harvesting from atmospheric air: A detailed review. *Sustainable Energy Technol Assess* 52: 102000. https://doi.org/10.1016/j.seta.2022.102000
3. Devesa R, Dietrich A (2018) Guidance for optimizing drinking water taste by adjusting mineralization as measured by total dissolved solids (TDS). *Desalination* 439: 147–154. https://doi.org/10.1016/j.desal.2018.04.017
4. Rai G, Rai G (1999) *Solar Energy Utilisation*. *Khhanna Publishers*. Available from: https://khannapublishers.in/index.php?route=product/product&product_id=165.
5. Kumaravel S, Nagaraj M, Bharathiraja G (2023) Experimental investigation on the performance analysis of blue metal stones and pebble stones as thermal energy storage materials in single slope solar still. *Mater Today: Proc* 77: 430–435. https://doi.org/10.1016/j.matpr.2022.11.100
6. Afolabi LO, Enweremadu CC, Kareem MW, et al. (2023) Experimental investigation of double slope solar still integrated with PCM nanoadditives microencapsulated thermal energy storage. *Desalination* 553: 116477. https://doi.org/10.1016/j.desal.2023.116477
7. Nwosu EC, Nwaji GN, Ononogbo C, et al. (2023) Effects of water thickness and glazing slope on the performance of a double-effect solar still. *Sci Afr* 21: e01777. https://doi.org/10.1016/j.sciaf.2023.e01777
8. Seralathan S, Chenna Reddy G, Sathish S, et al. (2023) Performance and exergy analysis of an inclined solar still with baffle arrangements. *Heliyon*, 9. https://doi.org/10.1016/j.heliyon.2023.e14807
9. Khan MZ (2022) Diffusion of single-effect vertical solar still fixed with inclined wick still: An experimental study. *Fuel* 329: 125502. https://doi.org/10.1016/j.fuel.2022.125502
10. Emran NY, Ahsan A, Al-Qadami EH, et al. (2022) Efficiency of a triangular solar still integrated with external PVC pipe solar heater and internal separated condenser. *Sustainable Energy Technol Assess* 52: 102258. https://doi.org/10.1016/j.seta.2022.102258

11. Banoqitah E, Sathyamurthy R, Moustafa EB, et al. (2023) Enhancement and prediction of a stepped solar still productivity integrated with paraffin wax enriched with nano-additives. *Case Stud Therm Eng* 49: 103215. https://doi.org/10.1016/j.csite.2023.103215
12. Davra D, Mehta P, Patel N, et al. (2024) Solar-enhanced freshwater generation in arid coastal environments: A double basin stepped solar still with vertical wick assistance study in northern Gujarat. *Sol Energy* 268: 112297. https://doi.org/10.1016/j.solener.2023.112297
13. Ahmed H, Najib A, Zaidi AA, et al. (2022) Modeling, design optimization and field testing of a solar still with corrugated absorber plate and phase change material for Karachi weather conditions. *Energy Rep* 8: 11530–11546. https://doi.org/10.1016/j.egyr.2022.08.276
14. Elashmawy M, Nafey A, Sharshir SW, et al. (2024) Experimental investigation of developed tubular solar still using multi-evaporator design. *J Cleaner Prod* 443: 141040. https://doi.org/10.1016/j.jclepro.2024.141040
15. Kabeel AE, Abdelgaied M, Attia MEH, et al. (2023) Performance enhancement of a conical solar still by optimizing inclination angle. *Sol Energy* 264: 112001. https://doi.org/10.1016/j.solener.2023.112001
16. Essa FA (2024) Aspects of energy, exergy, economy, and environment for performance evaluation of modified spherical solar still with rotating ball and phase change material. *J Energy Storage* 81: 110500. https://doi.org/10.1016/j.est.2024.110500
17. Abdullah A, Alqsair U, Aljaghtham MS, et al. (2023) Productivity augmentation of rotating wick solar still using different designs of porous breathable belt and quantum dots nanofluid. *Ain Shams Eng J* 14: 102248. https://doi.org/10.1016/j.asej.2023.102248
18. Abdullah A, Hadj-Taieb L, Omara Z, et al. (2023) Evaluating a corrugated wick solar still with phase change material, and external spiral copper heating coil. *J Energy Storage* 65: 107377. https://doi.org/10.1016/j.est.2023.107377
19. Sharshir SW, Farahat MA, Joseph A, et al. (2023) Comprehensive thermo-enviroeconomic performance analysis of a preheating-assisted trapezoidal solar still provided with various additives. *Desalination* 548: 116280. https://doi.org/10.1016/j.desal.2022.116280
20. Chauhan VK, Shukla SK (2023) Performance analysis of Prism shaped solar still using Black phosphorus quantum dot material and Lauric acid in composite climate: An experimental investigation. *Sol Energy* 253: 85–99. https://doi.org/10.1016/j.solener.2023.02.017
21. Shareef AS, Kurji HJ, Hamzah AH (2024) Modifying performance of solar still, by using slices absorber plate and new design of glass cover, experimental and numerical study. *Heliyon* 10: e24021. https://doi.org/10.1016/j.heliyon.2024.e24021
22. Alshamrani A (2023) Investigation of the performance of a double-glazing solar distiller with external condensation and nano-phase change material. *J Energy Storage* 73: 109075. https://doi.org/10.1016/j.est.2023.109075
23. Hameed HG (2022) Experimentally evaluating the performance of single slope solar still with glass cover cooling and square cross-section hollow fins. *Case Stud Therm Eng* 40: 102547. https://doi.org/10.1016/j.csite.2022.102547
24. Shatar NM, Sabri MFM, Salleh MFM, et al. (2023) Investigation on the performance of solar still with thermoelectric cooling system for various cover material. *Renewable Energy* 202: 844–854. https://doi.org/10.1016/j.renene.2022.11.105

25. Abdullah A, Hadj-Taieb L, Hikal M, et al. (2023) Enhancing a solar still's performance by preheating the feed water and employing phase-change material. *Alexandria Eng J* 77: 395–405. https://doi.org/10.1016/j.aej.2023.07.002
26. Abdullah A, Alawee WH, Mohammed SA, et al. (2023) Utilizing a single slope solar still with copper heating coil, external condenser, phase change material, along with internal and external reflectors—Experimental study. *J Energy Storage* 63: 106899. https://doi.org/10.1016/j.est.2023.106899
27. Dhivagar R, Shoeibi S, Parsa SM, et al. (2023) Performance evaluation of solar still using energy storage biomaterial with porous surface: An experimental study and environmental analysis. *Renewable Energy* 206: 879–889. https://doi.org/10.1016/j.renene.2023.02.097
28. Ebrahimpour B, Shafii MB (2022) Experimental evaluation of the effect of boulders and fines in biodegradable organic materials on the improvement of solar stills. *Sol Energy* 247: 453–467. https://doi.org/10.1016/j.solener.2022.10.045
29. Prasanna Y, Deshmukh SS (2022) Energy, exergy and economic analysis of an air cavity appended passive solar still of different basin material at varying depth. *Energy Sustainable Dev* 71: 13–26. https://doi.org/10.1016/j.esd.2022.09.008
30. Farghaly MB, Alahmadi RN, Sarhan H, et al. (2023) Experimental study of simultaneous effect of evacuated tube collectors coupled with parabolic reflectors on traditional single slope solar still efficiency. *Case Studies Therm Eng* 49: 103304. https://doi.org/10.1016/j.csite.2023.103304
31. Singh AK (2024) Analysis for optimized prerequisites of modified solar stills. *Heliyon* 10: e25804. https://doi.org/10.1016/j.heliyon.2024.e25804
32. Madhusudhan P, Devi NL, Kaliappan S, et al. (2023) Improving the productivity of the solar-based evaporative still (SBES) using the nano-coated absorber. *Mater Today: Proc*. https://doi.org/10.1016/j.matpr.2023.09.014
33. Abdullah AS, Omara ZM, Essa FA, et al. (2022) Enhancing trays solar still performance using wick finned absorber, nano-enhanced PCM. *Alexandria Eng J* 61: 12417–12430. https://doi.org/10.1016/j.aej.2022.06.033
34. Darbari B, Rashidi S (2022) Performance analysis for single slope solar still enhanced with multi-shaped floating porous absorber. *Sustainable Energy Technol Assess* 50: 101854. https://doi.org/10.1016/j.seta.2021.101854
35. Nehar L, Rahman T, Tuly S, et al. (2022) Thermal performance analysis of a solar still with different absorber plates and external copper condenser. *Groundwater Sustainable Dev* 17: 100763. https://doi.org/10.1016/j.gsd.2022.100763
36. Adam A, Saffaj N, Mamouni R (2023) Enhancement of adjusted solar still integrated with renewable energy: An experimental approach to recycling industrial wastewater. *Mater Today: Proc*. https://doi.org/10.1016/j.matpr.2023.07.056
37. Verma S, Das R, Mishra NK (2023) Concept of integrating geothermal energy for enhancing the performance of solar stills. *Desalination* 564: 116817. https://doi.org/10.1016/j.desal.2023.116817
38. Toosi SSA, Goshayeshi HR, Zahmatkesh I, et al. (2023) Experimental assessment of new designed stepped solar still with Fe_3O_4+ graphene oxide+ paraffin as nanofluid under constant magnetic field. *J Energy Storage* 62: 106795. https://doi.org/10.1016/j.est.2023.106795

39. Mandev E, Muratçobanoğlu B, Çelik A, et al. (2024) Improving solar still efficiency through integration of cellulose-based water absorbers and Peltier condensation unit. *Therm Sci Eng Prog* 49: 102475. https://doi.org/10.1016/j.tsep.2024.102475
40. Köse M, Akyürek EF, Afshari F (2025) Experimental investigation of horizontal solar stills using central container and transparent material as alternative to glass cover. *Heat Transfer Res* 56: 55–75. https://doi.org/10.1615/HeatTransRes.2024055441
41. Elsawy IM, Hamoda A, Sharshir SW, et al. (2023) Experimental study on optimized using activated agricultural wastes at hemispherical solar still for different types of water. *Process Saf Environ Prot* 177: 246–257. https://doi.org/10.1016/j.psep.2023.07.002
42. Dahab MA, Omara M, El-Dafrawy MM, et al. (2023) Thermo-economic performance enhancement of the hemispherical solar still integrated with various numbers of evacuated tubes. *Therm Sci Eng Prog* 42: 101922. https://doi.org/10.1016/j.tsep.2023.101922
43. Attia MEH, Hussein AK, Radhakrishnan G, et al. (2023) Energy, exergy and cost analysis of different hemispherical solar distillers: A comparative study. *Sol Energy Mater Sol Cells* 252: 112187. https://doi.org/10.1016/j.solmat.2023.112187
44. Beggas A, Abdelgaied M, Attia MEH, et al. (2023) Improving the freshwater productivity of hemispherical solar distillers using waste aluminum as store materials. *J Energy Storage* 60: 106692. https://doi.org/10.1016/j.est.2023.106692
45. Sharshir SW, Omara MA, Elsisi G, et al. (2023) Thermo-economic performance improvement of hemispherical solar still using wick material with V-corrugated basin and two different energy storage materials. *Sol Energy* 249: 336–352. https://doi.org/10.1016/j.solener.2022.11.038
46. Ghandourah E, Panchal H, Fallatah O, et al. (2022) Performance enhancement and economic analysis of pyramid solar still with corrugated absorber plate and conventional solar still: A case study. *Case Studies Therm Eng* 35: 101966. https://doi.org/10.1016/j.csite.2022.101966
47. Kumar A, Maurya A (2022) Experimental analysis and CFD modelling for pyramidal solar still. *Mater Today: Proc* 62: 2173–2178. https://doi.org/10.1016/j.matpr.2022.03.360
48. Abdullah A, Alawee WH, Mohammed SA, et al. (2023) Increasing the productivity of modified cords pyramid solar still using electric heater and various wick materials. *Process Saf Environ Prot* 169: 169–176. https://doi.org/10.1016/j.psep.2022.11.016
49. Sharshir SW, Rozza MA, Joseph A, et al. (2022) A new trapezoidal pyramid solar still design with multi thermal enhancers. *Appl Therm Eng* 213: 118699. https://doi.org/10.1016/j.applthermaleng.2022.118699
50. Omara Z, Alawee WH, Mohammed SA, et al. (2022) Experimental study on the performance of pyramid solar still with novel convex and dish absorbers and wick materials. *J Cleaner Prod* 373: 133835. https://doi.org/10.1016/j.jclepro.2022.133835
51. Sharshir SW, Rozza M, Elsharkawy M, et al. (2022) Performance evaluation of a modified pyramid solar still employing wick, reflectors, glass cooling and TiO_2 nanomaterial. *Desalination* 539: 115939. https://doi.org/10.1016/j.desal.2022.115939
52. Modi KV, Gamit AR (2022) Investigation on performance of square pyramid solar still using nanofluid and thermal energy storage material: An experimental and theoretical study. *J Cleaner Prod* 381: 135115. https://doi.org/10.1016/j.jclepro.2022.135115
53. Kajal G, Malik P, Garg H, et al. (2023) Thermophysical properties analysis of Al_2O_3, MgO and GO nanofluids with water for solar still. *Mater Today: Proc*.

54. Senthil Kumar S, Uma Mageswari SD, Meena M, et al. (2022) Effect of energy storage material on a triangular pyramid solar still operating with constant water depth. *Energy Rep* 8: 652–658. https://doi.org/10.1016/j.egyr.2022.10.203
55. Pandey H, Gupta NK (2022) Productivity analysis of pyramid solar still with solid clay pots. *Mater Today: Proc* 62: 4081–4085. https://doi.org/10.1016/j.matpr.2022.04.629
56. Asadabadi MJR, Sheikholeslami M (2022) Impact of utilizing hollow copper circular fins and glass wool insulation on the performance enhancement of pyramid solar still unit: An experimental approach. *Sol Energy* 241: 564–575. https://doi.org/10.1016/j.solener.2022.06.029
57. Alshqirate A, Awad AS, Al Alawin A, et al. (2023) Experimental investigation of solar still productivity enhancement of distilled water by using natural fibers. *Desalination* 553: 116487. https://doi.org/10.1016/j.desal.2023.116487
58. Ahmed ME, Abdo S, Abdelrahman M, et al. (2023) Finned-encapsulated PCM pyramid solar still–Experimental study with economic analysis. *J Energy Storage* 73: 108908. https://doi.org/10.1016/j.est.2023.108908
59. Sudhakar M, Sundar V, Farooq IU, et al. (2023) Experimental study on double slope (DSl) and triangular pyramid (TPy) solar stills under the influence of latent heat storage material (LHSM). *Mater Today: Proc*. https://doi.org/10.1016/j.matpr.2023.08.350
60. Bhoopathi R, Premnath A, Surendhar T, et al. (2023) Comparative study on pentagonal pyramid (PPy) and tubular (Tub) solar stills with thermal energy storage (TES). *Mater Today: Proc*. https://doi.org/10.1016/j.matpr.2023.08.336
61. Noman S, Manokar AM (2024) Experimental investigation of pistachio shell powder (bio-waste) to augment the performance of tubular solar still: Energy, exergy, and environmental analysis. *Desalination* 576: 117317. https://doi.org/10.1016/j.desal.2024.117317
62. Prasad AR, Harshith V, Harish R, et al. (2023) Investigating single sloped (SSl) and square pyramid (SPy) solar stills using phase changing material (PCM). *Mate Today: Proc*. https://doi.org/10.1016/j.matpr.2023.08.334
63. Dumka P, Mishra DR (2020) Performance evaluation of single slope solar still augmented with the ultrasonic fogger. *Energy* 190: 116398. https://doi.org/10.1016/j.energy.2019.116398
64. AbuShanab WS, Elsheikh AH, Ghandourah EI, et al. (2022) Performance improvement of solar distiller using hang wick, reflectors and phase change materials enriched with nano-additives. *Case Stud Therm Eng* 31: 101856. https://doi.org/10.1016/j.csite.2022.101856
65. Kandeal AW, Xu Z, Peng G, et al. (2022) Thermo-economic performance enhancement of a solar desalination unit using external condenser, nanofluid, and ultrasonic foggers. *Sustainable Energy Technol Assess* 52: 102348. https://doi.org/10.1016/j.seta.2022.102348
66. Sharshir SW, Kandeal A, Algazzar AM, et al. (2022) 4-E analysis of pyramid solar still augmented with external condenser, evacuated tubes, nanofluid and ultrasonic foggers: A comprehensive study. *Process Saf Environ Prot* 164: 408–417. https://doi.org/10.1016/j.psep.2022.06.026
67. El-Gazar E, Zahra W, Hassan H, et al. (2021) Fractional modeling for enhancing the thermal performance of conventional solar still using hybrid nanofluid: Energy and exergy analysis. *Desalination* 503: 114847. https://doi.org/10.1016/j.desal.2020.114847
68. Fath HE, El-Samanoudy M, Fahmy K, et al. (2003) Thermal-economic analysis and comparison between pyramid-shaped and single-slope solar still configurations. *Desalination* 159: 69–79. https://doi.org/10.1016/S0011-9164(03)90046-4

69. Kumar S, Tiwari G (2009) Life cycle cost analysis of single slope hybrid (PV/T) active solar still. *Appl Energy* 86: 1995–2004. https://doi.org/10.1016/j.apenergy.2009.03.005

AIMS Press